

When ‘more for others, less for self’ leads to co-benefits: a triad fMRI hyperscanning study

Le-Si Wang¹, Yi-Cing Chang², Shyhnan Liou¹, Ming-Hung Weng³, Der-Yow Chen², and Chun-Chia Kung²

¹National Cheng Kung University Institute of Creative Industries Design

²National Cheng Kung University Department of Psychology

³National Cheng Kung University Department of Economics

July 21, 2023

Abstract

Unselfishness is one of the admired facilitators for human group endeavors, especially in times of urgent calls for global collaboration. Despite its importance, the neural dynamics behind its formation is scarcely understood. With 26 triads interacting as turn-taking pairs in a coordination game, we investigated reciprocal interactions in this tri-fMRI hyperscanning experiment. The critical role of the right temporal-parietal junction (rTPJ) was examined by adopting both time- and frequency-domain analyses. For the former, in the successful versus failed “reciprocity” contrast, brain regions associated with the mirror neuron system (MNS) and the mentalizing system (MS) were identified. In addition, the differences of connectivity between the rTPJ (seed region) and the abovementioned network areas (e.g., the right Inferior Parietal Lobule, rIPL) were negatively correlated with the individual reward. These results both verified the experimental design, which favored ‘reciprocal’ participants/triads with larger gains, and supported the opposition of rTPJ (other-) vs. rIPL (self-concerned) areas during successful social exchanges. Furthermore, the cerebral synchronization of the rTPJs emerged between the interacting pairs, and the coupling between the rTPJ and the right Superior Temporal Gyrus (rSTG) was found between those interacting simultaneously with others of the same group. These coherence findings not only echoed our previous findings, but also reinforced the hypotheses of the rTPJ-rTPJ coupling underpinning simultaneous collaboration and the rTPJ-rSTG coupling for decontextualized shared meaning emergence. Taken together, these results support two of the multi-functions (other-concerning and decontextualizing) subserved by the rTPJ, and highlight its interaction with other self-concerning brain areas in reaching co-benefits.

Full title: When ‘more for others, less for self’ leads to co-benefits: a triad fMRI hyperscanning study

Short title: The triad fMRI hyperscanning on reciprocity

Le-Si Wang¹, Yi-Cing Chang², Shyhnan Liou¹, Ming-Hung Weng³ ¶, Der-Yow Chen^{2, 4} ¶, and Chun-Chia Kung^{2, 4} ¶

¹ Inst. of Creative Industries Design, National Cheng Kung University (NCKU), Tainan, Taiwan

² Dept. of Psychology, NCKU, Tainan, Taiwan

³ Dept. of Economics, NCKU, Tainan, Taiwan

⁴ Mind Research and Imaging Center (MRIC), Tainan, Taiwan

* Corresponding author

E-mail: cckung@kunglab-nckupsy.org

¶These authors contributed equally to this work.

Acknowledgments

We thank the NCKU Mind Research and Imaging Center (MRIC) at NCKU, the imaging center for integrated Body, Mind, and Culture research at NTU, and the Research Center for Mind, Brain, and Learning at NCCU for the generous equipment support for this cross-center collaboration. Special thanks go to all the hyperscanning teams for carrying out the experiment, as well as the preprocessing of fMRI data.

Abstract

Unselfishness is one of the admired facilitators for human group endeavors, especially in times of urgent calls for global collaboration. Despite its importance, the neural dynamics behind its formation is scarcely understood. With 26 triads interacting as turn-taking pairs in a coordination game, we investigated reciprocal interactions in this tri-fMRI hyperscanning experiment. The critical role of the right temporal-parietal junction (rTPJ) was examined by adopting both time- and frequency-domain analyses. For the former, in the successful versus failed “reciprocity” contrast, brain regions associated with the mirror neuron system (MNS) and the mentalizing system (MS) were identified. In addition, the differences of connectivity between the rTPJ (seed region) and the abovementioned network areas (e.g., the right Inferior Parietal Lobule, rIPL) were negatively correlated with the individual reward. These results both verified the experimental design, which favored ‘reciprocal’ participants/triads with larger gains, and supported the opposition of rTPJ (other-) vs. rIPL (self-concerned) areas during successful social exchanges. Furthermore, the cerebral synchronization of the rTPJs emerged between the interacting pairs, and the coupling between the rTPJ and the right Superior Temporal Gyrus (rSTG) was found between those interacting simultaneously with others of the same group. These coherence findings not only echoed our previous findings, but also reinforced the hypotheses of the rTPJ-rTPJ coupling underpinning simultaneous collaboration and the rTPJ-rSTG coupling for decontextualized shared meaning emergence. Taken together, these results support two of the multi-functions (other-concerning and decontextualizing) subserved by the rTPJ, and highlight its interaction with other self-concerning brain areas in reaching co-benefits.

Keywords: fMRI hyperscanning, Psychophysiological Interactions (PPI), coherence, collaboration, reciprocity

INTRODUCTION

Imagine you are in class and four people are arranged as a group to complete a task. You start to talk with the one next to you, and then maybe the one sitting facing you. After a run of talking, you may find yourself having better interactions with certain partners; meanwhile it is just too hard to keep your conversation flowing with someone. Somehow, each of your partners makes you feel something, and this leaves an impression of how you decide to react to them later on. Normally, the better interaction you have, the more willing you are to help with the task. By the definition of ‘help,’ it actually means you give and take in achieving an end, mutually. Phenomena of mutual interaction, experienced or expressed by each of two or more people or groups about the other, are ubiquitous. Social scientists may wonder if there is a difference that can be observed between pairs who are doing the same task at the same time but interacting with others. If yes, what is the neural difference between the partner who is sitting in front of you and talking to you, and the one who is sitting next to you and talking to another? How does your brain react to ‘good’ partners and ‘bad’ partners? As for neuroscientists, investigating social interactions in various contexts and revealing their neural correlates has never been more profound and implicative enough. In the present study, we are attempting to answer these questions regarding social interaction with three brains communicating pairwise.

Hyperscanning, simultaneously measuring the brain activity of multiple brains, allows the investigation of intra- and inter-brain neural relations in real-time dynamics (Czeszumski et al., 2020; Hari & Kujala, 2009; Scholkmann et al., 2013). Social neuroscience has developed research designs in hyperscanning in modalities other than fMRI, such as magnetoencephalography (MEG) (Holmes et al., 2023; Maysless et al.,

2019), electroencephalography (EEG) (Haresign et al., 2022; Turk et al., 2022), and functional near-infrared spectroscopy (fNIRS) (Nguyen et al., 2021; Zhang et al., 2023). Despite multiple brains interacting in sync, dyadic interactions and computations retain their fundamental roles in methodology and in research on the brain processes of social science. To progress toward real-life interactions, recent neuroscientific fMRI hyperscanning studies are mostly with dyads interacting with close-by or internet-connected scanners. Tasks to capture the emergent dynamics of simultaneous dual brain interactions include face-to-face interactions (such as gaze behavior) (Koike et al., 2019; Miyata et al., 2021), joint grips (Abe et al., 2019), coordination games (Goelman et al., 2019; Špiláková et al., 2019; Stolk et al., 2014; Wang et al., 2023; Yoshioka et al., 2021), natural events such as movie viewing (Schmälzle & Grall, 2020), and reciprocity in the ultimatum game (Shaw et al., 2018; Sperduti et al., 2014). Both the mirror neuron system (MNS) (Iacoboni & Dapretto, 2006) and the mentalizing system (MS) (Frith & Frith, 2006; Saxe, 2006) are indicated as playing vital roles in social interactions, especially in collaboration (Wang et al., 2018). For example, the Superior Temporal Gyrus (STG), the Inferior Parietal Lobule (IPL), the Inferior frontal gyrus (IFG), and the Precentral Gyrus, are among the brain networks during imitation (Heyes, 2001; Rizzolatti, 2005), an indispensable ingredients in positive rippling effects (Akgün et al., 2015; Barry, 2009); the TPJ and Precuneus are part of a mentalizing and default-mode network for interpreting cues of others (Hyatt et al., 2015; Li et al., 2014; Mars et al., 2012). Yet, as an old saying goes, “two’s company, three’s a crowd,” tri-MRI hyperscanning provides an unprecedented opportunity into the intricacies of group dynamics, given its varieties of three bi-directional, or even tri-directional, communications among group members.

Despite dyadic hyperscanning’s early onset (Montague et al., 2002), it was not until 2020 that we saw the first three-person fMRI hyperscanning study (Xie et al., 2020). In it, twelve triads engaged in a drawing task with collaborative and independent phases. Both GLM and intersubject correlation analyses (Hasson et al., 2004; Nummenmaa et al., 2018) indicated the critical role of rTPJ in the triadic collaborative interaction. As a likely second, in the present study we adopt both the time-domain, including GLM contrasts and Psychophysiological Interactions, or PPI, (O’Reilly et al., 2012), and frequency-domain coherence analysis (Wang et al., 2023) to reveal neural substrates of triadic social interactions. For the former, the aim is to investigate the neural differences between successful and failed reciprocity. We then adopted the successful and failed trials with reciprocity in the second stage of feedback time as our target trials. For the latter, we extend our prior work (Wang et al., 2023), a frequency-domain coherence analysis, into a 3-person internet-based hyperscanning (with the 4th sitting outside doing the same behavioral task) context (Sebanz et al., 2006; Vesper et al., 2016). Here, we focus on the stage of revealing whether the collaboration is successful (i.e., Stage 2 Feedback) because it is the shared period when the pairs check the results, build up the trust, and plan for the following trials. Note that there might be some nuances regarding unsuccessful, but not a failure to try to cooperate, and thus, may be underwritten by cooperative brain processes. This is not within the scope of the present study. Additionally, pairs win in two formats: the dyads could be kept in one dominant and the other submissive, or they could reciprocate with each other, which wins most in the end according to the experimental design. Lastly, when the inter-brain coherences were reported in the hyperscanning literature, the control conditions were mostly done by permuting individuals from different pairs (because of the exclusive within-pair interactions in dyads). In the present tri-fMRI study, however, the analyses of interpersonal coherence can be separated into several pairing combinations (see Methods for details), rendering at least three possible interpersonal couplings, thereby yielding multiple constraints of possible explanations.

What neural substrates, alone or together, contribute to meaningful interaction/coordination still holds scientists’ interest. From one brain to three, questions regarding subtle differences in mutual interaction can be empirically better understood. In summary, besides the technical advances in the tri-MRI implementation, reciprocity in collaboration and its meaning shared among dyads are elucidated in three analyses. These results generally suggest brain areas related to two essential networks in social interaction, the MNS and the MS. The present study plays an important contributor to the neuroscientific understanding of group collaboration, with implications for structuring co-benefits.

METHODS

Participants

Twenty-six triads of fMRI participants ($N_{\text{Male}} = 42$; $N_{\text{Female}} = 36$) were recruited from National Cheng Kung University (NCKU), National Taiwan University (NTU), and National Chengchi University (NCCU). NCKU is situated in southern Taiwan (Tainan), and NTU and NCCU in northern Taiwan (Taipei). All participants are native Taiwanese speakers, with normal or corrected-to-normal vision, and no history of psychiatric or neurological disorders. Participants gave informed consent and adhered to the guidelines and regulations approved by the NCKU Governance Framework for Human Research Ethics <https://rec.chass.ncku.edu.tw/en>, with the case number 106-254.

Experimental task

The experimental task was a revised coordination game (Farrell, 1988). Four players were playing at the same time, three inside the scanners and one outside for the behavior data only (Figure 1a). The participants took random turns playing with each other as a pair. The player roles, such as Player A, were fixed. Within a run, there were three 6-trial blocks, e.g., Block 1: A&B/C&D, Block 2: A&C/B&D, and Block 3: A&D/B&C. (Figure 1b), in which any assigned pair (e.g., Block 1: A&B/C&D) completed 6 trials in a row. There were 6 runs of such 3 (blocks) x 6 (trials) combinations, with the random order of pairings as $3! = 6$ (e.g., 123, 132, 213, 231, 312, and 321; one order for each run). Each run took about 7 to 8 minutes.

Each trial lasted about 19 seconds, containing two stages: the possible decision stage (preplay) and the actual decision stage (Figure 1c). Before each trial started, the screen showed with whom they would be interacting, e.g., “Interacting with Player B.” Next came the first, or communication, stage (**Stage 1 Decision**), where any given participant told the other player his/her choice by clicking the leftmost (‘1’) or the second leftmost key (‘2’), representing X and Y. The reward combination of (X, Y) was (1, 6), (6, 1), or (0, 0), suggesting that either one would choose the reward, 1 (or 6), and the other chooses 6 (or 1), or neither of them would get any reward. About 6 seconds later, the possible choices of both players were shown on the screen (**Stage 1 Feedback**). What they chose would be framed with a dotted rectangle, with one’s own choice in white and the other’s in another color. It is important to note that the possible/communicating choice in Stage 1 did not predicate the later actual choice. Participants in the second stage (**Stage 2 Decision**), after making their final decisions, would see their responses framed with a solid lined rectangle, with one’s own choice in white and the other’s in another color (**Stage 2 Feedback**), for up to 3 seconds. Three combinations to run statistics were Within-group Interacting Pairs (WIPs), Within-group Non-interacting Pairs (WNPs), and Between-group Permuted Pairs (BPPs) (Figure 1d).

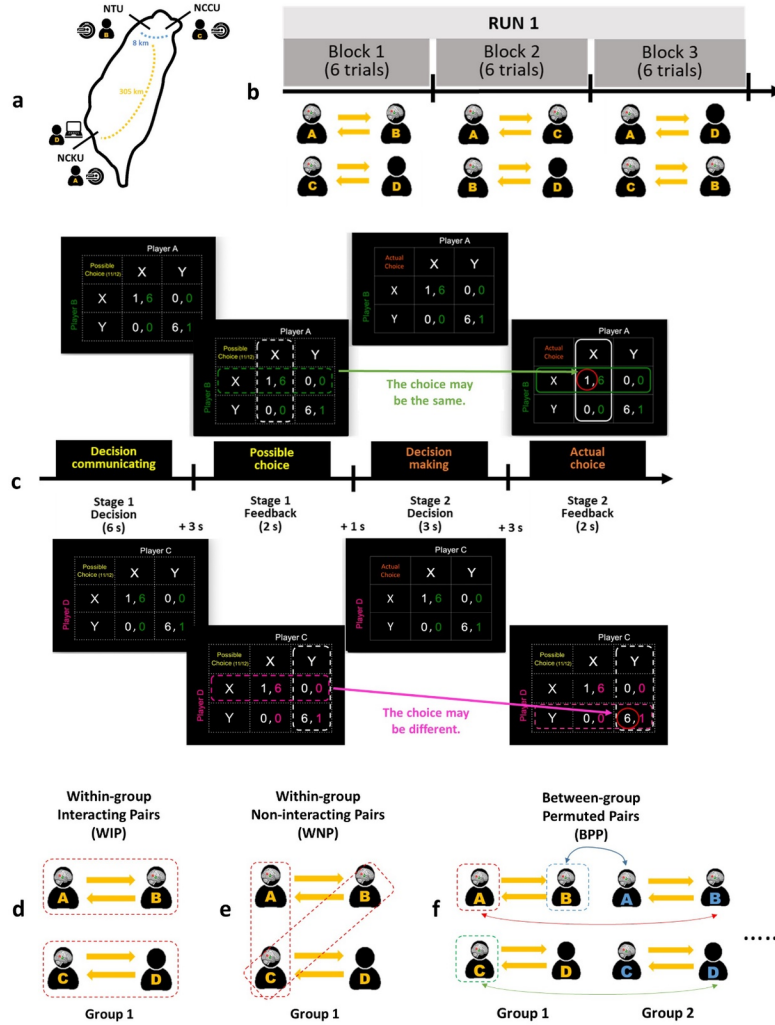


FIGURE 1. The experimental design (1a-1c) and the analysis conditions (1d-1g) of the present tri-fMRI hyperscanning study. (a) The fixed roles of the triads respectively in the three fMRI sites across Taiwan, National Cheng-Kung University (NCKU) as Player A, National Taiwan University (NTU) as Player B, and National Cheng-Chi University (NCCU) as Player C. NTU and NCCU are in northern Taiwan, 8 km away, while NCKU is in southern Taiwan, 305 km apart from NTU and NCCU. While Player A and Player B are interacting, Player C is interacting with Player D (who is outside of the NCKU MRI scanner). (b) There are 6 runs, 3 blocks in each run, and 6 trials in each block. Each run lasts about 7~8 minutes. In each trial (19 seconds), the four players are all playing the coordination game simultaneously, with two assigned pairs playing with each other (e.g., A&B+C&D), in different orders (e.g., A&C+B&D, and A&D+B&C). (c) The coordination game with preplay communications consists of two stages, each with a decision and a feedback for every player. The feedback in Stage 2 (17~19 s) is the target TR for coherence analysis because it is the actual choice (with rewards) revealing time for the interacting pairs to form trust, and to carry this successful history into the next trial. (d) **W**ithin-group**I**nteracting **P**airs (**WIP**) are

pairs that interact in the same group (e.g., A and B in Group 1 are the interacting pair). For fMRI analysis, there are 156 interacting pairs in total (3 players x 2 pairings [pairing with D is excluded] x 26 groups). **(e) Within-group Non-interacting Pairs (WNP)** are those who belong to the same group but interact with others at the same time (e.g., in Group 1, when A and B are interacting, A&C and B&C are non-interacting pairs.). There are 312 WNPs in total (3 players x 4 pairings x 26 groups). **(f) Between-group Permuted Pairs (BPP)** pair from different groups (e.g., A from Group 1 matches with B from Group 2, or A from Group 1 matches with C from Group 2, etc.). There are 3,900 BPPs in total (3 players x 50 pairings x 26 groups).

fMRI data acquisition and preprocessing

The fMRI images were acquired simultaneously in three MRI scanners, one in NCKU Tainan, another in NTU Taipei, and the other in NCCU Taipei. NCKU is about 305 km apart from NTU and NCCU, and NTU is about 8 km apart from NCCU (Figure 1a). The MRI scanner at NCKU Mind Research and Imaging Center is a 3-Tesla General Electric Discovery MR750 (GE Medical Systems, Waukesha, WI), equipped with an 8-ch head coil. Whole-brain functional scans were acquired with a T2* EPI (TR = 2 s, TE = 33 ms, flip angle = 90°, 40 axial slices, voxel size = 3.5 x 3.5 x 3 mm³). High-resolution T1-weighted structural scans were acquired using a 3D fast spoiled grass (FSPGR) sequence (TR = 7.65 ms, TE = 2.93 ms, inversion time = 450 ms, FA = 12deg, 166 sagittal slices, voxel size = 0.875 x 0.875 x 1 mm³). Another fMRI scanner, which is located at NTU (Imaging Center for the Body, Mind, and Culture Research) is a 3-Tesla PRISMA (Siemens, Erlangen, Germany) scanner equipped with a 20-channel phased array coil. Whole-brain functional scans were acquired with a T2*-weighted EPI (TR = 2 s, TE = 24 ms, flip angle = 87deg, 36 axial slices, voxel size = 3 x 3 x 3 mm³). High-resolution T1-weighted structural scans were acquired using a MP-RAGE (TR = 2.0 s, TE = 2.3 ms, inversion time = 900 ms, FA = 8deg, 192 sagittal slices with 0.938 x 0.938 x 0.94 mm³ voxels without an interslice gap). The other scanner fMRI scanner, which is located at NCCU (Taiwan Mind & Brain Imaging Center) is a 3-Tesla MAGNETOM Skyra (Siemens, Erlangen, Germany) scanner equipped with a 20-channel phase array coil. Whole-brain functional scans were acquired with a T2*-weighted EPI (TR = 2 s, TE = 24 ms, flip angle = 87deg, 36 axial slices, voxel size = 3 x 3 x 3 mm³). High-resolution T1-weighted structural scans were acquired using an MP-RAGE (TR = 2.53 s, TE = 3.3 ms, inversion time = 1100 ms, FA = 7deg, 192 sagittal slices with 1 x 1 x 1 mm³ voxels without an interslice gap). Although these three scanners vary in quality and parameters, the highly overlapping histograms in rTPJ beta Figure 2a) and coherence value (Figure 2b) among NCKU (MR750), NTU (Prisma), and NCCU (Skyra) underpin our data-pooling later.

The fMRI data were preprocessed and analyzed using BrainVoyagerQX v. 2.6 (Brain Innovation, Maastricht, The Netherlands) and NeuroElf v1.1 (<https://neuroelf.net>). After slice timing correction, functional images were corrected for head movements using the six-parameter rigid transformations, aligning all functional volumes to the first volume of the first run. High-pass temporal filtering (with the default BVQX option of GLM-Fourier basis set at 2 cycles per deg, but no spatial smoothing) was applied. The resulting functional data were co-registered to the anatomical scan via initial alignment (IA) and final alignment (FA), and then both functional (T2* EPI data) and anatomical (T1 structural data) files were transformed into the Talairach space.

General linear model (GLM) and psychophysiological interactions (PPI) analyses

The GLM estimated each participant' brain activations and compared the contrasts of interests. In order to make predictions for the blood-oxygen level dependent (BOLD) responses of various periods during the coordinating interaction, we divided each trial into four phases: 1) Stage 1 Decision, 2) Stage 1 Feedback, 3) Stage 2 Decision, and 4) Stage 2 Feedback. To test if the BOLD responses were different in successful and failed reciprocity trials (i.e., Successful vs. Failed), contrast analysis was performed on all subjects. Alphasim was adopted to correct the error rate of multiple comparisons among whole-brain voxels. Under the threshold of familywise error (FEW) $p < 0.05$, the minimum cluster size with a threshold of $p < 0.01$ was defined as 44 voxels.

In addition to the GLM contrast analysis, the psychophysiological interactions (PPI) analysis was applied to examine differences of functional connectivity between the seed region of interest (i.e., the $rTPJ_{seed}$) and target ROIs. The $rTPJ_{seed}$ was heavily involved in the ToM, attention, and social networks (Koster-Hale & Saxe, 2013; Premack & Woodruff, 1978; Wang et al., 2018; Young et al., 2010). In a social cognition review (Babiloni & Astolfi, 2014), the rTPJ activation has been consistently identified during tasks related to the process of information. In another review of more than 200 fMRI studies (Van Overwalle, 2009), the rTPJ has its crucial role in transient mental inferences about other people. A recent review of patients with damaged rTPJ even suggests its role in predicting others (Masina et al., 2022). The $rTPJ_{seed}[54, -55, 22]$ was downloaded from neurosynth.org, comprising 103 published studies, with z scores 8.82 (corresponding to $FDR=0.01$, with ‘association test’ option). It is a functional mask with 239 voxels. In addition, to investigate the individual differences in the total reward under the contrast of successful and failed reciprocal interactions, and such relationship with their functional connectivity, participants’ total reward was correlated with their connectivity differences to reveal behavior-relevant brain networks. All correlation analyses were conducted using Matlab and JASP (<https://jasp-stats.org/>).

Data preparation for the frequency-domain coherence analysis

The procedure of converting a jittered event-related fMRI dataset into a format ready for coherence analysis was reported earlier (Wang et al., 2023). This time-frequency coherence analysis was adopted here to estimate inter-brain couplings. As coherence requires long duration in a predictable manner, we created a periodicity (18 s), targeting only on the feedback stage and lasting approximately as long as a run of the experiment ([?] 19 s). These beta-concatenated time series were extracted by iteratively estimating feedback-related blood oxygenation level-dependent responses of each trial. Details are as follows.

First, the feedback period of any given trial (here the second stage) was used (Figure 2a). Next, the protocol (or .prt file) of an fMRI run (totally 6 runs), along with the voxel time series, was created. Then, a single deconvolutional GLM was created, with 9 stick-like extensions (Figure 2b). This method allowed a least-square separation of the target trial, from which the whole brain beta series were independently estimated subsequently for the 9 TRs following the feedback-initiated event, with a finite impulse response (FIR) function (Turner et al., 2012). The feedback time, revealing the result of the actual choices from the 17th second to the 19th, was the time the dyad built up the impressions about each interacting partner. All the 9-TR volumes from each trial (6 in one run) and for the 6 runs were concatenated, resulting in 324 volumes (9 TRs x 6 trials x 6 runs), as the periodic data format ready was for coherence analysis (Figure 2c).

Time-frequency seed-based coherence analyses were conducted across pairs of choice by using the FieldTrip toolbox (<https://www.fieldtriptoolbox.org/>). The $rTPJ_{seed}$ was the same as adopted in PPI analysis. Coherence analyses were performed between one’s (e.g., A) rTPJ to another’s (e.g., B) whole brain, and B’s rTPJ to A’s whole brain, and then averaged across a dyad, and then across all 26 groups under specific pairings (detailed later in 2.6) (Figure 2d). The groupwise whole-brain mask was derived from averaging over the whole 78 participants. The coherence operation yielded 162 frequency bins, out of $0.5 \text{ (fMRI sampling frequency)} / 324 / 2$ (Nyquist equation) = 162 frequency bins. Since we estimated 9 beta series (each for 2 seconds), the 36th ($1/18 \text{ s} = 0.0556 \text{ Hz}$) frequency bin would be the frequency of interest. The regions with high coherence were separately mapped (Figure 2e). For the result presentation, the condition-wise whole-brain mapping was shown via NeuroElf.

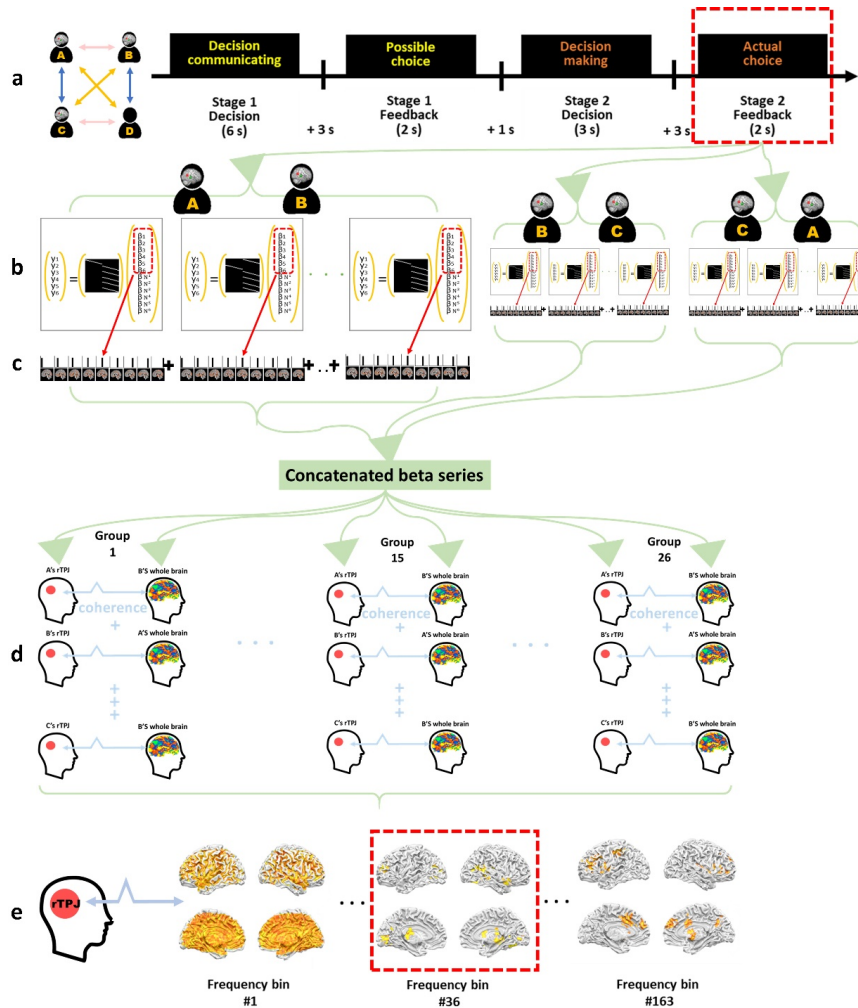


FIGURE 2. The schematic procedure of converting an fMRI dataset into a format ready for coherence analysis. (a) Player A, B, C, and D take turns interacting as pairs at the same time. Player D is outside the scanner. “Feedback” is defined as the time in the second stage of a trial when the actual choices of the pairs are made, to the end of the 2-s period in each trial. (b) A single deconvolutional GLM is created, with 9 stick-like extensions for each of the two regressors (“target_trial” and “other_trials”). This method allows a least-square separation of the target trial, from which the whole brain beta series are independently estimated subsequently for the 9 TRs following the feedback-initiated event; (c) Concatenating all the 9 TRs from each trial, resulting in 324 volumes [9 TRs x 6 trials (each run for each pair) x 6 runs] for each pair, as the periodic data format ready for coherence analysis. (d) The rTPJ is chosen as the seed ROI of the current study for the interpersonal seed-brain coherence analysis. The ROI beta series are extracted from the previously concatenated beta series and applied to the whole brain of the other subject. (e) The regions coupled with the rTPJ at the target frequency bin, the 36th ($1/18\text{ s} = 0.0556\text{ Hz}$), are separately mapped.

Various subgroups, indices and pairing combinations for analyses

As an alternative method to characterize individual behavioral characteristics, k-means cluster analyses, a module in JASP with the Silhouette optimization algorithm (Rousseeuw, 1987), was further implemented, yielding 3 subgroups:

1. **reciprocal:** taking turns for the bigger reward, $n = 49$;
2. **dominant:** choosing the bigger reward in 2 consecutive trials, $n = 14$;
3. **submissive:** choosing the smaller reward in back-to-back trials, $n = 15$.

The descriptive statistics of each subgroup were shown in the Supplementary Table S1. These subgroup labels were instrumental in the brain-behavior connectivity analyses.

Two kinds of behavioral indices were devised: individual-wise and pair/dyad-wise. For the individual-based behavioral indices, each player interacted with the other three players and had 6 consecutive interactions with one player in a run, 6 runs in total; out of 6 runs, there were 35 times of alternation because the first interaction/trial was not included ($35 \text{ times/trials} \times 3 \text{ other players} = 105 \text{ trials}$). Three kinds of trial could be derived out of the total 105 trial pairs for each participant:

a) successful trials: Either Player A or B won the bigger reward. **b) failed trials:** Both Player A and B chose the same (bigger or smaller) reward, ending up both winning zero. **c) successful trials with reciprocity:** Player A won the bigger reward, and then B won the bigger reward in the next trial, or vice versa; **d) successful trials without reciprocity:** Either Player A or B won the bigger reward for two trials in a row;

Three individual-based indices were calculated based on these three kinds of trial pairs:

1. **the reciprocity index:** defined as the number of successful trials with the winner of the bigger reward alternated (e.g., AB or BA), divided by the 105 calculable trials;
2. **the greed index:** defined by the number of successful trials without reciprocity, such as one (e.g., AA or CC) winning consecutive bigger rewards;
3. **the total reward:** defined as the sum of money each participant earned in the whole experimental session.

The 2nd set of, or pair-based, indices are:

pairwise success rate: defined as the pairs successfully winning the reward, regardless of which player won the bigger/smaller amount;

pairwise reciprocity rate: defined as the pair taking turns in getting the bigger reward.

Details of pairing for coherence analyses are as follows:

1. **Within-group Interacting Pairs (WIPs)** . The WIPs are pairs within the same group and are interacting at the same time. For example, when Player A is interacting with Player B (i.e., A&B) and Player C is interacting with Player D (i.e., C&D) in Block 1, A&B and C&D are two interacting pairs. For a given experimental group (3 scanned + 1 behavioral), there are 3 players X 2 pairings X 26 groups = 156 combinations.
2. **Within-group Non-interacting Pairs (WNPs)** . To use the A&B/C&D pairings above for example, A&C is the non-interacting pair (for Player D is outside the fMRI, thus with no neural data). For a given experimental group, there are 3 players X 4 pairings X 26 groups = 312 combinations.
3. **Between-group Permuted Pairs (BPPs)** . BPPs are pairings of players from different groups, e.g., A from Group 1 to B/C from Group 2, etc. ($3 \text{ players} \times 50 \text{ pairings} \times 26 \text{ groups} = 3,900 \text{ combinations}$).

Independent two-sample t-tests were carried out for various ROIs on the three pairings (WIPs, WNPs, and BPPs) to determine whether they were different distinct populations.

RESULTS

Behavioral results

In the individual level, the reciprocity index, the mean percentage of successful trials with the winner of the bigger reward alternated was $56.47 \pm 17.8\%$ (the reciprocity index), the mean percentage of successful trials without reciprocity was $4.80 \pm 4.18\%$ (the greed index), and the average sum of money each participant earned in the whole experimental session was $\$290.1 \pm 44.1$ NTD.

The results of the pair-based indices indicate \sout{on} average 76.4% (=27.5/ out of 36, or 6 in 6 runs) of the trials the pairs successfully won the reward (the pairwise success rate), and \sout{on} average 73.8% (=25.8/35 possible alternations from each dyad) the pair took turns in getting the bigger reward (pairwise reciprocity rate). The pairwise success rate was significantly correlated with the pairwise alternation rate ($r = 0.921$, $p < 0.001$), which suggests that the majority of players soon learned to coordinate with three others, without being given explicit instructions and being strangers throughout (i.e., participants were drawn from three different universities). These also reflect the effectiveness of the study design, which enabled the participants to follow their natural tendencies.

The homogeneity checks of tri-fMRI data

As a sanity check, the triad-fMRI data from the three sites (NCKU with GE MR750, NTU with Siemens Prisma, and NCCU with MAGNETOM Skyra), after the same preprocessing steps and coherence preparations \sout{(Figure 2)}, were compared in the seed-rTPJ betas and the rTPJ-rTPJ coherence values (Supplementary Figure S1). The results show that these data were highly overlapping on the major dependent measures. In other words, despite different raw image values and scanning parameters from each vendor, the three sites' fMRI data remained homogenous and comparable, ready for the interpersonal coherence analyses.

GLM contrasts and PPI analyses

As the first pass of most fMRI studies, the GLM contrast between the successful and failed reciprocal trials, on the 2nd feedback phase, were identified and compared. Here, only the stage of revealing the final result (i.e., Stage 2 Feedback) was chosen as the dyads shared this period to see whether the collaboration/coordination was (reciprocally) successful for reward. This feedback stage helped the dyads with trust-building for the following trials. Two additional reasons are as follows: a) collinearity and b) the extension and replication of our previous study (Wang et al., 2023). In our experiment design, the events of the parameters estimated were fixed. These highly correlated events (i.e., Stage 1 Decision is always followed by Stage 1 Feedback, then Stage 2 Decision, and finally Stage Feedback 2 Feedback) might result in being biased. Consequently, the GLMs were separate for each stage (only 'Stage 2 feedback' was adopted in the following analysis), instead of a single GLM run with all 4 onsets. Second, we adopted Stage 2 Feedback in our previous analysis for coherence. This study was aimed to extend and replicate our previous one; thus, the same period of time was employed for further analysis.

Figure 3a represents the brain regions with significant activations in the [Successful > Failed trials] contrast. As shown in the Supplementary Table S2, the contrast [Successful trials > Failed trials] in the second stage of feedback seven activated clusters are identified, including the right Precentral Gyrus (rPG), the right Posterior Cingulate, the right Caudate, the left Middle Temporal Gyrus, the left Middle Frontal Gyrus, the left Medial Frontal Gyrus, and the left Inferior Frontal Gyrus. To examine the brain-behavior relationship, we calculated the correlation between the three indices (i.e., greed, and total reward) and the [Successful trials > Failed trials] contrast. No ROI was found correlated.

In addition to GLM contrast analysis, the rTPJ_{seed} downloaded from Neurosynth.com was used as the seed region to examine the target regions where their functional connectivity was significantly stronger in the successful vs. failed reciprocity trials. In the second feedback phase, the bilateral Precentral Gyri, bilateral Inferior Frontal Gyrus, bilateral Insula, right Medial Frontal Gyrus, left Inferior Parietal Lobule, right Cingulate Gyrus, left Middle Frontal Gyrus, right Postcentral Gyrus and left Precuneus were identified as more negatively functionally connected with rTPJ in the successful trials than in the failed trials (see the Supplementary Table S3). The target regions were also mapped in Figure 3b. To examine the brain-behavior relationship, we calculated the correlation between the three indices (i.e., reciprocity, greed, and total reward) and the [Successful trials > Failed trials] contrast. Only the right Sub-gyral was found correlated

with reciprocity (see the supplementary Table S4).

We further employed connectivity-based correlations with individual total reward. To investigate the underlying network differences with their individual total reward in the successful vs. in the failed trials, the $rTPJ_{seed}$ connectivity was further examined. The results showed negative functional connectivity in the right postcentral gyrus, right Angular Gyrus, and right Inferior Parietal Lobule when the participants successfully reciprocated with their pairmates (see Figure 3c and the Supplementary Table S5). These results indicated that the lower the functional connectivities between the hub areas of different sub-networks, such as attention/memory and self-other awareness areas between $rTPJ$ - $rIPL$ and $-rAG$, the higher reproductive success.

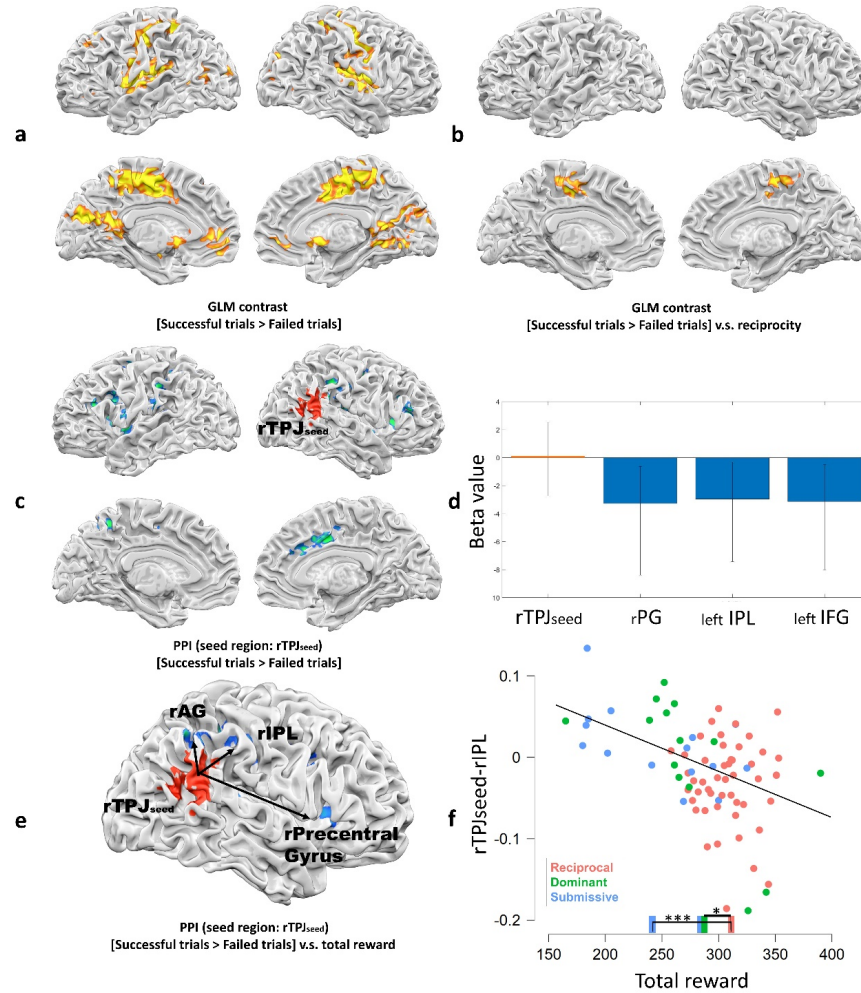


FIGURE 3. (a) The GLM [successful trials > failed trials] contrast in the second stage of feedback reveals activated clusters, such as the rPG . (b) The right Sub-gyral was found correlated with the individual

reciprocity index in the [successful trials > failed trials] contrast. The other two indices (greed and total reward) were not shown correlated with any brain regions. **(c)** The PPI results showed more negative functional connectivity in the MNS (such as the rPG, the left IPL, and the bilateral IFG,) with the rTPJ_{seed} in the successful reciprocity trials. **(d)** The bar graph shows the beta values extracted from some of the regions shown in **(d)** for illustration purposes only. These regions are negatively correlated with the seed region, the rTPJ [from left to the right: rTPJ_{seed} ($M = 0.13, SD = 1.07$), rPG ($M = -3.29, SD = 0.51$), left IPL ($M = -2.98, SD = 0.38$), and left IFG -3 ($M = -3.15, SD = 0.43$)]. **(e)** The rTPJ_{seed}-rPG, -rAG, and -rIPL connectivities, correlated with individual total reward indicates that one's rTPJ (thinking of others) activity increases, with the depressed activity of the right PG for coordinated action, and the right IPL and right AG for relating themselves and detecting incongruence, in the successful reciprocity trials. See further detailed interpretation in Discussion. **(f)** The scatter plot shows the correlations between the total reward and one of the three ROIs (the right IPL chosen for illustration purposes; See the other two in Supplementary Figure S3) found via PPI. The three types of participants are: reciprocal (red), dominant (green), and submissive (blue). The bars on the x axle show the mean total reward of the three types: reciprocal (NT\$ 307.82), dominant (NT\$ 274), and submissive (NT\$ 247.28). The scatter plot suggests the reciprocal individuals (in red) with the most reward (reciprocal-dominant, $p = 0.014$; reciprocal-submissive, $p < 0.001$) and negative connectivity between the rTPJ_{seed} and the right IPL identified from PPI.

rTPJ_{seed}-to-whole brain frequency-domain coherence

Comparisons among various pairing combinations

The rTPJ_{seed}-whole brain interpersonal coherence of the WIPs in the second stage feedback time is shown in the Supplementary Table S6. Brain regions show significant coherence with the rTPJ_{seed} during the event of feedback time under the cluster k-threshold of 40 voxels and the applied map threshold of 0.215. Furthermore, we compared the 36th frequency bin with the rest, excluding the first 3 bins, and the 35th/the 37th; the peak of 36th bin is higher than the rest by 1.5 of the standard errors. The ROIs with significant coherence with the rTPJ_{seed} are the rTPJ and among others. In the WNPs, the rTPJ_{seed} are significantly coupled with the rSTG and others under the cluster k-threshold of 40 voxels and the applied map threshold of 0.215 (see Supplementary Table S7). Also the peak of the 36th frequency bin is higher than the rest by 1.5 standard errors.

To further investigate inter-regional couplings, Figure 4 shows the coherence spectra between rTPJ_{seed}-rTPJ_p (posterior right TPJ) in the WIPs pairs (Figure 4a) and rTPJ_{seed}-rSTG in the WNPs (Figure 4b). The independent two-sample t-tests are applied among every possible pair at the 36th frequency bin. The rTPJ_{seed}-rTPJ_p coherence value of the WIPs is stronger than those of the WNPs and BPPs (all $ps < 0.001$). The rTPJ_{seed}-rSTG coherence value of the WNPs (in yellow) is stronger than those of the WIPs ($p < 0.016$) and BPPs ($p < 0.001$).

We ran the same analyses and applied the same peak threshold (the 36th frequency bin is higher than the rest by 1.5 standard errors) on the first feedback (in the planning stage) to compare with the results of the second feedback stage in coherence. Brain regions show significant coherence with the rTPJ_{seed} during the event of first feedback time under the cluster k-threshold of 40 voxels and the applied map threshold of 0.225. Bilateral Lingual Gyri, the left PG, and the right Precuneus are identified in the WIPs. In the WNPs, the bilateral Lingual Gyri were found coupling with the rTPJ_{seed} during the event of first feedback time under the cluster k-threshold of 40 voxels and the applied map threshold of 0.22 (see Figure 4c and Supplementary Table S8-9).

As the interacting pairs had real interactions with each other in the same group, we calculated the three neural differences in coherence when 1) reciprocal people interacted with reciprocal partners and 2) with non-reciprocal ones (the dominant and submissive types). Furthermore, we calculated the coherence values among 3) the non-reciprocal pairs. After applying the stringent threshold (the peak of the designated frequency bin, the 36th, should be higher than the rest by 1.5 standard errors), we found the left TPJ and right IFG coupled with the rTPJ among the reciprocal pairs (under the cluster k-threshold of 40 voxels and the applied

map threshold of 0.228). When the reciprocal individuals interacted with the non-reciprocal partners, no coupling was found with the rTPJ. As for the non-reciprocal pairs, their left IFG and the right amygdala were in sync with the rTPJ (under the cluster k-threshold of 40 voxels and the applied map threshold of 0.226). (See Figure 4d-e and the Supplementary Table S10-11)

To examine the brain-behavior relationship, we calculated the correlation between the coherence values of the regions found coupled with the rTPJ in the WIP. No significant results were shown (see the Supplementary Table S12).

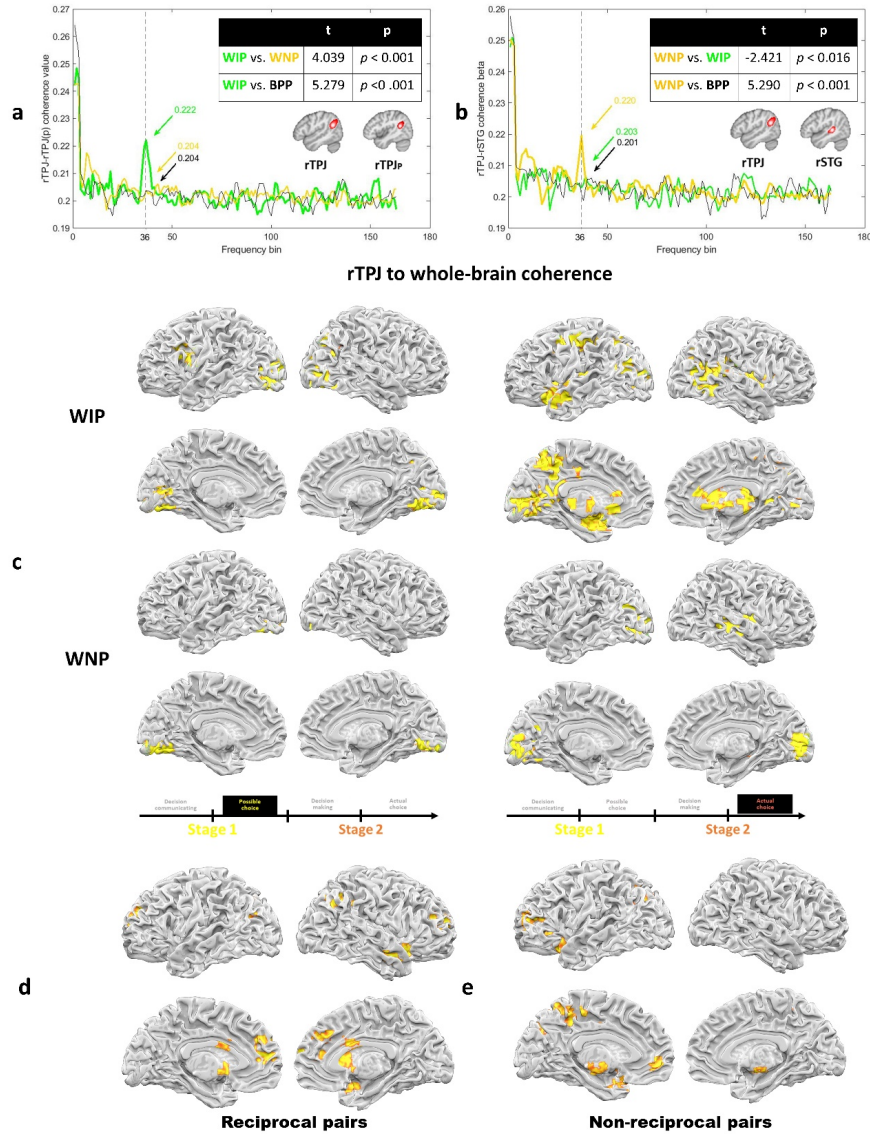


FIGURE 4. The comparisons of inter-regional couplings.(a) The coherence spectra between $rTPJ_{seed}$ - $rTPJ_p$ and (b) The $rTPJ_{seed}$ - $rSTG$ in the conditions of the within-group interacting pairs (WIP), within-group non-interacting pairs (WNP), within-group permuted pairs (WPP), and between-group permuted pairs (BPP). The brain maps show the seed (left) and the target (right) regions on the 36th frequency bin (out of $324/2 = 162$ bins, or the target frequency 0.0556 Hz, or 1/18 s), under the coherence threshold of

0.215 and the cluster threshold of 40 voxels (FWE $p < .05$ corr.). This bin corresponds to the average trial frequency, or the concatenated event frequency (beta series built by combining 9 betas, every 2 s/ 1 TR, after the trial feedback time). The spectra of the WIPs are shown in green, WNP in yellow, and the BPPs in black. The independent two-sample t-tests are applied among every possible pair at the 36th frequency bin. **(c)** The rTPJ_{seed} to whole-brain coherence maps of the WIP and WNP in the two stages of feedback periods, respectively. In the first stage of feedback (planning stage), the WIP and WNP have bilateral Lingual Gyri linked to processing vision and episodic memory. In the second feedback (decision stage), more couplings with the rTPJ can be observed in the WIP, while the rTPJ-STG coupling of the WNP outstands, compared to the WNP map in Stage 1. **(d)** When the reciprocal pairs are interacting with each other, their left TPJ and right IFG are coupled with the rTPJ_{seed} in the second feedback. **(e)** The non-reciprocal pairs yield rTPJ- amygdala and -left IFG couplings when interacting together.

Discussion

Collaboration through reciprocity is evident in many social contexts, as humans share and connect with each other from interactions. In the present study, we investigated whether brain circuitry was identified as relevant for reciprocal collaborations through social learning in a coordination game. First, our behavioral results showed that successful collaboration was correlated with reciprocity, and the reciprocal participants and pairs earned the most reward. This reflects that the utmost successful interaction of the present study lies in reciprocity. Second, in the neural level, the MNS and the MS involving coordination-, reward-, and decision-related regions known for cooperation tasks were identified. Many abovementioned regions were both found in our time-domain (i.e., GLM and PPI) and frequency-domain (i.e., coherence) analyses. Furthermore, the rTPJ was suggested to play its dual roles in social interaction with the brain regions related to other/self-concern (intrapersonally) and meaning-emergence (interpersonally). In sum, given its critical placement in mentalizing, the rTPJ is likely to participate in multiple functions through the present three-person hyperscanning.

‘ Our GLM results confirmed that significant activity in the mirror neuron related regions, including the Precentral Gyrus, the Posterior Cingulate, the IFG, and the TPJ when successful coordination was achieved. The MNS has been known for imitating actions as shared communication (Schmidt et al., 2021). In previous review studies, activity in the MNS is often significantly recruited in joint action (Mu et al., 2018; Pacherie & Dokic, 2006; Sebanz & Knoblich, 2009). In human social cognition, the MNS plays its crucial role of understanding of action and intentional agency (Gallese et al., 1996; Rizzolatti, 2005; Rizzolatti et al., 2001) and the emergence of language (Arbib & Bota, 2003; Arbib, 2002; Mu et al., 2018; Rizzolatti & Arbib, 1998). In addition, regions related to execution and observation of actions, such as the IFG, the Middle Frontal Gyrus, and the Medial Frontal Gyrus (Molenberghs et al., 2012; Takeuchi et al., 2013), were also involved in succeeding reciprocity. Since our task is a revised coordination game, far more complicated than merely imitating actions, successful dyadic interactions lie in careful decision-related processes. One study also suggests that the mirror neuron system may not just help participant mirror actions but process intentionally complementary or opposing actions (Campbell et al., 2018). In order to achieve reciprocity for final utmost reward, previous trial interactions should be observed and taken into consideration for the following trial. In particular, the role of the left IFG in action understanding and processing intention is examined (Pobric & Hamilton, 2006) as a necessity in making a perceptual judgment about people’s actions. This may result in the recruited activity of the IFG, especially, found in all of our three analyses. Lastly, activity associated with reward/reinforcement in the Caudate increased as the dyads were mutually benefited in a row. This explains how the pairs commonly reacted to reward when the successful results were revealed during the second feedback stage and continued to follow reciprocal interaction. We further ran correlations between the [successful trials > failed trials] condition and the three indices (i.e., reward, greed, and reciprocity), and the right Sub-gyral in the motor cortex was strongly correlated with an individual’s reciprocity. The Sub-gyral has been suggested for its role in coordination (Swinnen et al., 2010; Ullén et al., 2003). Not surprisingly, a person’s successful interaction with the other, which often leads to reciprocity in the present experiment, lies in good coordination in this motor-related area.

Our PPI analyses indicated individual differences in successful and failed reciprocity trials in functional connectivity between the rTPJ (seed region) and the other regions, which are similar to our GLM results. Interestingly, lower functional connectivity was found with the rTPJ, which is known for a role in theory of mind for mentalizing others' intentions (Saxe & Kanwisher, 2003). Our results may elucidate how the rTPJ interacts with other regions associated with the MNS and MS. One hypothesis is that the rTPJ may fire more strongly and thus suppress the other self-related regions. Findings of the previous studies on the MNS and MS suggest a complementary or collaborative role of the two networks during social exchanges (Sperduti et al., 2014; Van Overwalle & Baetens, 2009; Wang et al., 2018), while Frith and Frith (2006) concluded that the MS is superior to the MNS for communicative intent. In our coordination game, the task is not simply about winning cooperatively, but reciprocally. Pairs do not just imitate each other's behavior. They have to figure out how to reach mutual benefits and meanwhile how to gain more reward for themselves. This mentalizing process may recruit more activity of the rTPJ and less activity of self-related regions. One cannot be too greedy or too generous (or submissive), for both of the strategies result in less amount of final reward than acting reciprocal. This may explain why regions related to self-related aspects of experience, including the Precuneus, insula and IPL (Cabanis et al., 2013; Chiao et al., 2009; Harada et al., 2020; Ray et al., 2010; Shi et al., 2021), exhibited negative correlations with the rTPJ.

Further PPI analyses were conducted to investigate the relationship between the functional connectivity and the total reward of individuals. Regions associated with coordination/MNS (the rPG), attention reorientation, and self-perception (the rAG and rIPL) (Corbetta et al., 2008; Igelström & Graziano, 2017; Mitchell, 2008) were shown lower functional connectivity with the rTPJ_{seed} when an individual's total reward increased in the contrast of successful trials versus failed trials. In other words, the bigger the contrast between the rTPJ and the ROIs mentioned above exhibits, the less total reward one earns. As discussed above, the rPG for imitation in the MNS and the IPL for self-other differentiation may be more suppressed when the rTPJ needs to be more resource-allocated for mentalizing for others to achieve reciprocity. Moreover, the AG and IPL are activated especially in predicting valid cues (Corbetta et al., 2002; Vossel et al., 2006), which results in less effort in successful trials for the cues as predicted. A gradient descent functional connectivity between these ROIs and the rTPJ negatively correlated with the total reward was also found among the dynamics of the subgroups (submissive > dominant > reciprocal) (see Figure 3f and the Supplementary Figure S3). That is, a bigger ROI-rTPJ contrast but a smaller amount of the total reward was yielded among the submissive participants. This can be interpreted that those who acted submissive might be less coordinated and less attentive than the reciprocal participants, and suppressing their desire in reward might exhaust their mind when they were fulfilling others (higher activity of the rTPJ in mentalizing others).

Regarding our frequency-domain results, two neural couplings of interest, the rTPJ-rTPJ and rTPJ-rSTG, were found highly consistent with social interactions. The first connectivity of the rTPJ-rTPJ emerging in the interacting pairs can be seen to draw on constant tracking of the other's intention, mentalizing, and continuous communications for achieving success in collaboration. This coupling also implies common operation with attention (Igelström & Graziano, 2017) and social attributions (Saxe & Kanwisher, 2003). Recently, the rTPJ has been suggested to act as an interface of self- and other-related or external- or internal-triggered information processing (Bzdok et al., 2013). In particular, the rTPJ_p is associated with social reasoning in a theory-of-mind experiment design (Krall et al., 2015; Kubit & Jack, 2013). Previous experiments invoking face-to-face joint attention with one participant in autism spectrum disorder (Redcay et al., 2012), and in gaze-following of monkeys (Kamphuis et al., 2009) and humans (Laube et al., 2011), or two participants (Abe et al., 2019; Bilek et al., 2015; Koike et al., 2019), have shown activation of the rTPJ_p for extra attention to track social cues. In the present study, this rTPJ-rTPJ_p neural synchrony based on social information integration and social behavior formation is in line with the literature regarding the coordination of self- and other-behavior (Carter & Huettel, 2013; Corbetta et al., 2008; Geng & Vossel, 2013). We further compared this feedback in the decision stage (Stage 2 Feedback) to that in the planning stage (Stage 1 Feedback). The results again strongly support our original and previous results that the rTPJ-rTPJ and -rSTG couplings can be found only in the second/decision/final feedback, not in the feedback in the planning stage. Another interesting result is that similar couplings (the rTPJ coupled with the bilateral Lingual Gyri, linked to

processing vision and episodic memory) were found among the pairs who were interacting (WIPs) and those who were doing the same task in the same group as the WIP but with other partners (WNPs). In addition, the right Precuneus, involved in self-referential processing, imagery, and memory, was identified in sync with the rTPJ only in the WIP in the planning stage, compared with the WNP also in the planning stage and the WIP in the decision stage.

Our results of the rSTG's roles in social cognition and perception are in good agreement with the existing knowledge. A few hyperscanning fMRI studies, which also implemented the interpersonal coherence measures, reported similar findings. For example, Wang et al. (2023) demonstrated the similar rTPJ-rTPJ_p coupling when participants competed for the whole reward (i.e., thus highly attentive), the rTPJ-rSTG coupling when participants collaborated and split the reward (97.5% trusting the partner, thus less attention demand required). In the Token-Coordination task (Stolk et al., 2014), similar rSTG-rSTG coherence between highly collaborative pairs, implicates such coupling as the foundation of meaning (Stolk et al., 2016). In the present study, being able to compute among three pairing groups (i.e., interacting, non-interacting, and permuted), we would like to propose the idea of decontextualization of the rTPJ-rSTG coupling as the shared meaning for the common good. When pairs are in the context of interacting, their rTPJs synchronize to mentalize each other. While they are interacting with their pairmates, the rTPJs of theirs are coupled with the rSTGs of the other two groupmates who are interacting with their pairmates at the same time. The shift of the rTPJ-rTPJ coupling between pairmates (while interacting with each other) and the rTPJ-rSTG coupling between groupmates (while interacting with another in the same group), compared to the baseline (the permuted results), highlights the formation of decontextualization in the rTPJ-rSTG coupling. As trials go on, the rTPJ-rSTG coupling can only be explained to be for shared goal orientation, or simply understanding the game rules. While more resources may be allocated in the rTPJ for thinking about the real interacting partner, the interpersonal rTPJ-rSTG coupling is found in sync between groupmates despite the same coordination game and the simultaneous interacting time among all of them. In short, we would like to refer to the rTPJ-rSTG coupling as the understanding of the shared meaning. Here the interpretation of this coupling can be referred as to the meaning of the common good, which is that 'reciprocity leads to better individual and group gain.' This neural substrate serves as a mutual understanding of abstraction, which is relevant to how human languages were formed and shared among a group of people as human beings are the symbolic species (Deacon, 1997).

By using the behavioral data, we classified subjects into three types (reciprocal, dominant, and submissive). We further calculated the differences in coherence values when subjects of different types were paired or when subjects of uniform type were paired. This may help to understand the mental processing of different types of subjects yielding different oscillation synchronization. The TPJ was found between the reciprocal pairs, and the IFG was identified among the reciprocal pairs and the non-reciprocal types (dominant and/or submissive). These brain regions are often associated with for action understanding and processing intention as we discussed a lot above. Compared with the reciprocal pairs, the non-reciprocal pairs had negative emotion arousal in their right amygdala in sync with the rTPJ. This is an interesting finding which echoes our real-life scenario that there may be bad blood or hard feelings between the non-reciprocal pairs.

To date, the analysis for spatio-temporal dynamics of hyperscanning data does not have standard computational models to follow (Kelsen et al., 2022). Still, we tested if the evoked neural responses in the frequency domain were temporally coherent. The results were all found insignificant, suggesting that the effect size of frequency-domain coherence is relatively miniscule, rendering the transformation into the time domain almost non-existent. Small or null temporal effects in the ROIs were derived from the analyses of the frequency domain. For example, in the interacting pairs, the rTPJ_{seed}-rTPJ_p time-course correlation was 0.039 and its beta correlation was 0.005. Besides more spatio-temporal analysis comparisons, we suggest that interpersonal connectivities may be better for frequency-domain analysis, while the time domain analysis is better for intra-personal correlations. Moreover, two implications are concluded: 1) publication bias and 2) future methodological requirements for more than two brains. First, due to different temporal and spatial resolution of tools (e.g., EEG and fMRI), analyses vary. Take the fMRI studies for example. Most studies adopt time domain analyses, such as GLM, PPI, and multivariate pattern analysis because of fMRI's poor temporal

resolution for frequency domain analysis (e.g., coherence). Comparisons with temporal-spatial analysis are barely tested, not to mention being reported, for its unfavorable insignificant results. Some may propose to collect two kinds of data from EEG-fMRI or MEG-fMRI. Again, the scanner threshold within 3 mm head motion flexibility may result in the ecological setting issue. Therefore, it still remains incomplete but explorable between spatio-temporal methods. Second, our limitation here is that the triad data were not analyzed in a triad method. Instead, the contrasts and connectivities between pairs were employed. We acknowledge that we have not been able to come up with new analyses to test the correlations and connectivities among three participants. As we all know, there will be a long way to validate the three- or even four-way hyperscanning results by adopting more than pairwise correlations. In fact, even though dyadic fMRI hyperscanning has been adopted for more than two decades, the methods are still diverse and debatable. Besides, previous studies employed EEG and fNIRS with multiple participants interacting in sync and also adopted pairwise methods, such as coherence. Interpersonal couplings are always averaged across pairs; there is no difference statistically to average across triads. For future possibilities, analyses can be run by three or more brains simultaneously, as the results can support more for interpreting multi-brain interactions (Babiloni & Astolfi, 2014; Hamilton, 2021).

Aside from individual's mind and brain states to characterize social neuroscience in the past, the burgeoning works of such hyperscanning, both in implementation and analysis perspectives, provide novel insights into this much needed (in both theory and applications) field of study. Reviewing histories and looking ahead, we are constantly reminded that the future of human races, facing the challenges of global crises in environment, welfare, resource management and so forth, will only be solved by collective actions. The prerequisites of collaborations among organizations of various scales, from families to countries, are assurances of mutual attitudes throughout the processes. In cases where any sign of disconfirming evidence arises, the social reciprocity might fall and collapse along a downward spiral. This is why in addition to the protection from supervising organizations or sound policies, players' mutual guarantee through trust and reciprocity plays a vital role in long-term social mutual benefits.

References

- Abe, M. O., Koike, T., Okazaki, S., Sugawara, S. K., Takahashi, K., Watanabe, K., & Sadato, N. (2019). Neural correlates of online cooperation during joint force production. *NeuroImage* , *191* , 150-161.
- Akgün, A. E., Keskin, H., Ayar, H., & Erdoğan, E. (2015). The influence of storytelling approach in travel writings on readers' empathy and travel intentions. *Procedia-Social and Behavioral Sciences* , *207* , 577-586.
- Arbib, M., & Bota, M. (2003). Language evolution: neural homologies and neuroinformatics. *Neural Networks* , *16* (9), 1237-1260.
- Arbib, M. A. (2002). The mirror system, imitation, and the evolution of language. *Imitation in animals and artifacts* , *229* , 38.
- Babiloni, F., & Astolfi, L. (2014). Social neuroscience and hyperscanning techniques: past, present and future. *Neuroscience & Biobehavioral Reviews* , *44* , 76-93.
- Barry, A. M. (2009). Mirror neurons: How we become what we see. *Visual Communication Quarterly* , *16* (2), 79-89.
- Bilek, E., Ruf, M., Schäfer, A., Akdeniz, C., Calhoun, V. D., Schmahl, C., Demanuele, C., Tost, H., Kirsch, P., & Meyer-Lindenberg, A. (2015). Information flow between interacting human brains: Identification, validation, and relationship to social expertise. *Proceedings of the National Academy of Sciences* , *112* (16), 5207-5212.
- Bzdok, D., Laird, A. R., Zilles, K., Fox, P. T., & Eickhoff, S. B. (2013). An investigation of the structural, connectional, and functional subspecialization in the human amygdala. *Human brain mapping* , *34* (12), 3247-3266.

- Cabanis, M., Pyka, M., Mehl, S., Müller, B. W., Loos-Jankowiak, S., Winterer, G., Wölwer, W., Musso, F., Klingberg, S., & Rapp, A. M. (2013). The precuneus and the insula in self-attributional processes. *Cognitive, Affective, & Behavioral Neuroscience* , 13 , 330-345.
- Campbell, M. E., Mehrkanoon, S., & Cunnington, R. (2018). Intentionally not imitating: Insula cortex engaged for top-down control of action mirroring. *Neuropsychologia* , 111 , 241-251.
- Carter, R. M., & Huettel, S. A. (2013). A nexus model of the temporal–parietal junction. *Trends in cognitive sciences* ,17 (7), 328-336.
- Chiao, J. Y., Harada, T., Komeda, H., Li, Z., Mano, Y., Saito, D., Parrish, T. B., Sadato, N., & Iidaka, T. (2009). Neural basis of individualistic and collectivistic views of self. *Human brain mapping* , 30 (9), 2813-2820.
- Corbetta, M., Kincade, J. M., & Shulman, G. L. (2002). Neural systems for visual orienting and their relationships to spatial working memory. *Journal of cognitive neuroscience* , 14 (3), 508-523.
- Corbetta, M., Patel, G., & Shulman, G. L. (2008). The reorienting system of the human brain: from environment to theory of mind. *Neuron* , 58 (3), 306-324.
- Czeszumski, A., Eustergerling, S., Lang, A., Menrath, D., Gerstenberger, M., Schuberth, S., Schreiber, F., Rendon, Z. Z., & König, P. (2020). Hyperscanning: a valid method to study neural inter-brain underpinnings of social interaction. *Frontiers in Human Neuroscience* ,14 , 39.
- Deacon, T. W. (1997). *The symbolic species: The co-evolution of language and the brain* . WW Norton & Company.
- Farrell, J. (1988). Communication, coordination and Nash equilibrium. *Economics Letters* , 27 (3), 209-214.
- Frith, C. D., & Frith, U. (2006). The neural basis of mentalizing. *Neuron* , 50 (4), 531-534.
- Gallese, V., Fadiga, L., Fogassi, L., & Rizzolatti, G. (1996). Action recognition in the premotor cortex. *Brain* , 119 (2), 593-609.
- Geng, J. J., & Vossel, S. (2013). Re-evaluating the role of TPJ in attentional control: contextual updating? *Neuroscience & Biobehavioral Reviews* , 37 (10), 2608-2620.
- Goelman, G., Dan, R., Stöbel, G., Tost, H., Meyer-Lindenberg, A., & Bilek, E. (2019). Bidirectional signal exchanges and their mechanisms during joint attention interaction—A hyperscanning fMRI study. *NeuroImage* , 198 , 242-254.
- Hamilton, A. F. d. C. (2021). Hyperscanning: beyond the hype. *Neuron* , 109 (3), 404-407.
- Harada, T., Mano, Y., Komeda, H., Hechtman, L. A., Pornpattananangkul, N., Parrish, T. B., Sadato, N., Iidaka, T., & Chiao, J. Y. (2020). Cultural influences on neural systems of intergroup emotion perception: An fMRI study. *Neuropsychologia* , 137 , 107254.
- Haresign, I. M., Phillips, E., Whitehorn, M., Goupil, L., Noreika, V., Leong, V., & Wass, S. (2022). Measuring the temporal dynamics of inter-personal neural entrainment in continuous child-adult EEG hyperscanning data. *Developmental Cognitive Neuroscience* ,54 , 101093.
- Hari, R., & Kujala, M. V. (2009). Brain basis of human social interaction: from concepts to brain imaging. *Physiological reviews* , 89 (2), 453-479.
- Hasson, U., Nir, Y., Levy, I., Fuhrmann, G., & Malach, R. (2004). Intersubject synchronization of cortical activity during natural vision. *Science* , 303 (5664), 1634-1640.
- Heyes, C. (2001). Causes and consequences of imitation. *Trends in cognitive sciences* , 5 (6), 253-261.

- Holmes, N., Rea, M., Hill, R. M., Boto, E., Leggett, J., Edwards, L. J., Rhodes, N., Shah, V., Osborne, J., & Fromhold, T. M. (2023). Naturalistic hyperscanning with wearable magnetoencephalography. *Sensors* , 23 (12), 5454.
- Hyatt, C. J., Calhoun, V. D., Pearlson, G. D., & Assaf, M. (2015). Specific default mode subnetworks support mentalizing as revealed through opposing network recruitment by social and semantic fMRI tasks. *Human brain mapping* , 36 (8), 3047-3063.
- Iacoboni, M., & Dapretto, M. (2006). The mirror neuron system and the consequences of its dysfunction. *Nature Reviews Neuroscience* , 7 (12), 942-951.
- Igelström, K. M., & Graziano, M. S. (2017). The inferior parietal lobule and temporoparietal junction: a network perspective. *Neuropsychologia* , 105 , 70-83.
- Kamphuis, S., Dicke, P. W., & Thier, P. (2009). Neuronal substrates of gaze following in monkeys. *European Journal of Neuroscience* , 29 (8), 1732-1738.
- Kelsen, B. A., Sumich, A., Kasabov, N., Liang, S. H., & Wang, G. Y. (2022). What has social neuroscience learned from hyperscanning studies of spoken communication? A systematic review. *Neuroscience & Biobehavioral Reviews* , 132 , 1249-1262.
- Koike, T., Sumiya, M., Nakagawa, E., Okazaki, S., & Sadato, N. (2019). What makes eye contact special? Neural substrates of on-line mutual eye-gaze: a hyperscanning fMRI study. *Eneuro* , 6 (1).
- Koster-Hale, J., & Saxe, R. (2013). Theory of mind: a neural prediction problem. *Neuron* , 79 (5), 836-848.
- Krall, S. C., Rottschy, C., Oberwelland, E., Bzdok, D., Fox, P. T., Eickhoff, S. B., Fink, G. R., & Konrad, K. (2015). The role of the right temporoparietal junction in attention and social interaction as revealed by ALE meta-analysis. *Brain Structure and Function* , 220 (2), 587-604.
- Kubit, B., & Jack, A. I. (2013). Rethinking the role of the rTPJ in attention and social cognition in light of the opposing domains hypothesis: findings from an ALE-based meta-analysis and resting-state functional connectivity. *Frontiers in Human Neuroscience* , 7 , 323.
- Laube, I., Kamphuis, S., Dicke, P. W., & Thier, P. (2011). Cortical processing of head-and eye-gaze cues guiding joint social attention. *NeuroImage* , 54 (2), 1643-1653.
- Li, W., Mai, X., & Liu, C. (2014). The default mode network and social understanding of others: what do brain connectivity studies tell us. *Frontiers in Human Neuroscience* , 8 , 74.
- Mars, R. B., Neubert, F.-X., Noonan, M. P., Sallet, J., Toni, I., & Rushworth, M. F. (2012). On the relationship between the “default mode network” and the “social brain”. *Frontiers in Human Neuroscience* , 6 , 189.
- Masina, F., Pezzetta, R., Lago, S., Mantini, D., Scarpazza, C., & Arcara, G. (2022). Disconnection from prediction: a systematic review on the role of right temporoparietal junction in aberrant predictive processing. *Neuroscience & Biobehavioral Reviews* , 138 , 104713.
- Mayseless, N., Hawthorne, G., & Reiss, A. L. (2019). Real-life creative problem solving in teams: fNIRS based hyperscanning study. *NeuroImage* , 203 , 116161.
- Mitchell, J. P. (2008). Activity in right temporo-parietal junction is not selective for theory-of-mind. *Cerebral Cortex* , 18 (2), 262-271.
- Miyata, K., Koike, T., Nakagawa, E., Harada, T., Sumiya, M., Yamamoto, T., & Sadato, N. (2021). Neural substrates for sharing intention in action during face-to-face imitation. *NeuroImage* , 233 , 117916.
- Molenberghs, P., Cunnington, R., & Mattingley, J. B. (2012). Brain regions with mirror properties: a meta-analysis of 125 human fMRI studies. *Neuroscience & Biobehavioral Reviews* , 36 (1), 341-349.

- Montague, P. R., Berns, G. S., Cohen, J. D., McClure, S. M., Pagnoni, G., Dhamala, M., Wiest, M. C., Karpov, I., King, R. D., & Apple, N. (2002). Hyperscanning: simultaneous fMRI during linked social interactions. In (Vol. 16, pp. 1159-1164): Citeseer.
- Mu, Y., Cerritos, C., & Khan, F. (2018). Neural mechanisms underlying interpersonal coordination: a review of hyperscanning research. *Social and Personality Psychology Compass* , 12 (11), e12421.
- Nguyen, T., Schleihauf, H., Kungl, M., Kayhan, E., Hoehl, S., & Vrtička, P. (2021). Interpersonal neural synchrony during father-child problem solving: an fNIRS hyperscanning study. *Child development* ,92 (4), e565-e580.
- Nummenmaa, L., Lahnakoski, J. M., & Glerean, E. (2018). Sharing the social world via intersubject neural synchronisation. *Current Opinion in Psychology* , 24 , 7-14.
- O'Reilly, J. X., Woolrich, M. W., Behrens, T. E., Smith, S. M., & Johansen-Berg, H. (2012). Tools of the trade: psychophysiological interactions and functional connectivity. *Social Cognitive and Affective Neuroscience* , 7 (5), 604-609.
- Pacherie, E., & Dokic, J. (2006). From mirror neurons to joint actions. *Cognitive systems research* , 7 (2-3), 101-112.
- Pobric, G., & Hamilton, A. F. d. C. (2006). Action understanding requires the left inferior frontal cortex. *Current Biology* ,16 (5), 524-529.
- Premack, D., & Woodruff, G. (1978). Does the chimpanzee have a theory of mind? *Behavioral and brain sciences* , 1 (4), 515-526.
- Ray, R. D., Shelton, A. L., Hollon, N. G., Matsumoto, D., Frankel, C. B., Gross, J. J., & Gabrieli, J. D. (2010). Interdependent self-construal and neural representations of self and mother. *Social Cognitive and Affective Neuroscience* , 5 (2-3), 318-323.
- Redcay, E., Kleiner, M., & Saxe, R. (2012). Look at this: the neural correlates of initiating and responding to bids for joint attention. *Frontiers in Human Neuroscience* , 169.
- Rizzolatti, G. (2005). The mirror neuron system and its function in humans. *Anatomy and embryology* , 210 (5-6), 419-421.
- Rizzolatti, G., & Arbib, M. A. (1998). Language within our grasp. *Trends in neurosciences* , 21 (5), 188-194.
- Rizzolatti, G., Fogassi, L., & Gallese, V. (2001). Neurophysiological mechanisms underlying the understanding and imitation of action. *Nature Reviews Neuroscience* , 2 (9), 661-670.
- Rousseeuw, P. J. (1987). Silhouettes: a graphical aid to the interpretation and validation of cluster analysis. *Journal of computational and applied mathematics* , 20 , 53-65.
- Saxe, R. (2006). Uniquely human social cognition. *Current opinion in neurobiology* , 16 (2), 235-239.
- Saxe, R., & Kanwisher, N. (2003). People thinking about thinking people: The role of the temporo-parietal junction in "theory of mind". *NeuroImage* , 19 (4), 1835-1842.
- Schmälzle, R., & Grall, C. (2020). The coupled brains of captivated audiences. *Journal of Media Psychology* .
- Schmidt, S. N., Hass, J., Kirsch, P., & Mier, D. (2021). The human mirror neuron system—A common neural basis for social cognition? *Psychophysiology* , 58 (5), e13781.
- Scholkmann, F., Holper, L., Wolf, U., & Wolf, M. (2013). A new methodical approach in neuroscience: assessing inter-personal brain coupling using functional near-infrared imaging (fNIRI) hyperscanning. *Frontiers in Human Neuroscience* , 7 , 813.

- Sebanz, N., Bekkering, H., & Knoblich, G. (2006). Joint action: bodies and minds moving together. *Trends in cognitive sciences* , 10 (2), 70-76.
- Sebanz, N., & Knoblich, G. (2009). Prediction in joint action: What, when, and where. *Topics in cognitive science* , 1 (2), 353-367.
- Shaw, D. J., Czekóová, K., Staněk, R., Mareček, R., Urbánek, T., Špalek, J., Kopečková, L., Řezáč, J., & Brázdil, M. (2018). A dual-fMRI investigation of the iterated Ultimatum Game reveals that reciprocal behaviour is associated with neural alignment. *Scientific reports* , 8 (1), 10896.
- Shi, G., Li, X., Zhu, Y., Shang, R., Sun, Y., Guo, H., & Sui, J. (2021). The divided brain: Functional brain asymmetry underlying self-construal. *NeuroImage* , 240 , 118382.
- Sperduti, M., Guionnet, S., Fossati, P., & Nadel, J. (2014). Mirror Neuron System and Mentalizing System connect during online social interaction. *Cognitive processing* , 15 (3), 307-316.
- Špiláková, B., Shaw, D. J., Czekóová, K., & Brázdil, M. (2019). Dissecting social interaction: dual-fMRI reveals patterns of interpersonal brain-behavior relationships that dissociate among dimensions of social exchange. *Social Cognitive and Affective Neuroscience* , 14 (2), 225-235.
- Stolk, A., Noordzij, M. L., Verhagen, L., Volman, I., Schoffelen, J.-M., Oostenveld, R., Hagoort, P., & Toni, I. (2014). Cerebral coherence between communicators marks the emergence of meaning. *Proceedings of the National Academy of Sciences* , 111 (51), 18183-18188.
- Stolk, A., Verhagen, L., & Toni, I. (2016). Conceptual alignment: How brains achieve mutual understanding. *Trends in cognitive sciences* , 20 (3), 180-191.
- Swinnen, S. P., Vangheluwe, S., Wagemans, J., Coxon, J. P., Goble, D. J., Van Impe, A., Sunaert, S., Peeters, R., & Wenderoth, N. (2010). Shared neural resources between left and right interlimb coordination skills: the neural substrate of abstract motor representations. *NeuroImage* , 49 (3), 2570-2580.
- Takeuchi, H., Taki, Y., Sassa, Y., Hashizume, H., Sekiguchi, A., Fukushima, A., & Kawashima, R. (2013). Brain structures associated with executive functions during everyday events in a non-clinical sample. *Brain Structure and Function* , 218 , 1017-1032.
- Turk, E., Endevelt-Shapira, Y., Feldman, R., van den Heuvel, M. I., & Levy, J. (2022). Brains in sync: Practical guideline for parent–infant EEG during natural interaction. *Frontiers in psychology* , 13 , 833112.
- Turner, B. O., Mumford, J. A., Poldrack, R. A., & Ashby, F. G. (2012). Spatiotemporal activity estimation for multivoxel pattern analysis with rapid event-related designs. *NeuroImage* , 62 (3), 1429-1438.
- Ullén, F., Forssberg, H., & Ehrsson, H. H. (2003). Neural networks for the coordination of the hands in time. *Journal of Neurophysiology* , 89 (2), 1126-1135.
- Van Overwalle, F. (2009). Social cognition and the brain: a meta-analysis. *Human brain mapping* , 30 (3), 829-858.
- Van Overwalle, F., & Baetens, K. (2009). Understanding others' actions and goals by mirror and mentalizing systems: a meta-analysis. *NeuroImage* , 48 (3), 564-584.
- Vesper, C., Schmitz, L., Safra, L., Sebanz, N., & Knoblich, G. (2016). The role of shared visual information for joint action coordination. *Cognition* , 153 , 118-123.
- Vossel, S., Thiel, C. M., & Fink, G. R. (2006). Cue validity modulates the neural correlates of covert endogenous orienting of attention in parietal and frontal cortex. *NeuroImage* , 32 (3), 1257-1264.
- Wang, L.-S., Cheng, J.-T., Hsu, I.-J., Liou, S., Kung, C.-C., Chen, D.-Y., & Weng, M.-H. (2023). Distinct cerebral coherence in task-based fMRI hyperscanning: cooperation versus competition. *Cerebral Cortex* , 33 (2), 421-433.

Wang, M.-Y., Luan, P., Zhang, J., Xiang, Y.-T., Niu, H., & Yuan, Z. (2018). Concurrent mapping of brain activation from multiple subjects during social interaction by hyperscanning: a mini-review. *Quantitative imaging in medicine and surgery* , 8 (8), 819.

Xie, H., Karipidis, I. I., Howell, A., Schreier, M., Sheau, K. E., Manchanda, M. K., Ayub, R., Glover, G. H., Jung, M., & Reiss, A. L. (2020). Finding the neural correlates of collaboration using a three-person fMRI hyperscanning paradigm. *Proceedings of the National Academy of Sciences* , 117 (37), 23066-23072.

Yoshioka, A., Tanabe, H. C., Sumiya, M., Nakagawa, E., Okazaki, S., Koike, T., & Sadato, N. (2021). Neural substrates of shared visual experiences: a hyperscanning fMRI study. *Social Cognitive and Affective Neuroscience* , 16 (12), 1264-1275.

Young, L., Dodell-Feder, D., & Saxe, R. (2010). What gets the attention of the temporo-parietal junction? An fMRI investigation of attention and theory of mind. *Neuropsychologia* , 48 (9), 2658-2664.

Zhang, W., Qiu, L., Tang, F., & Li, H. (2023). Affective or cognitive interpersonal emotion regulation in couples: an fNIRS hyperscanning study. *Cerebral Cortex* , 33 (12), 7960-7970.

Hosted file

point-by-point reponse.docx available at <https://authorea.com/users/641983/articles/656005-when-more-for-others-less-for-self-leads-to-co-benefits-a-triad-fmri-hyperscanning-study>